

Phospholipid membrane restructuring induced by saposin C: a topographic study using atomic force microscopy

Hong Xing You^{a,*}, Lei Yu^a, Xiaoyang Qi^b

^aDepartment of Cell Biology, Neurobiology, and Anatomy, University of Cincinnati College of Medicine, 3125 Eden Ave, Cincinnati, OH 45267-0521, USA

^bThe Division of Human Genetics, Children's Hospital Research Foundation, 3333 Burnet Ave, Cincinnati, OH 45229-3039, USA

Received 13 July 2001; accepted 16 July 2001

First published online 25 July 2001

Edited by Guido Tettamanti

Abstract The enzymatic activity of glucosylceramidase depends on the presence of saposin C (Sap C) and acidic phospholipid-containing membranes. In order to delineate the mechanism underlying Sap C stimulation of the enzyme activity, it is important to understand how Sap C interacts with phospholipid membranes. We studied the dynamic process of Sap C interaction with planar phospholipid membranes, in real time, using atomic force microscopy (AFM). The phospholipid membrane underwent restructuring upon addition of Sap C. The topographic characteristics of the membrane restructuring include the appearance of patch-like new features, initially emerged at the edge of phospholipid membranes and extended laterally with time. Changes in the image contrast of the phospholipid membrane observed after the Sap C addition indicate that a new phase of lipid-protein structure has formed during membrane restructuring. The process of membrane restructuring is dynamic, commencing shortly after Sap C addition, and continuing throughout the duration of AFM imaging (about 30 min, sometimes over 1 h). This study demonstrated the potential of AFM real-time imaging in studying protein-membrane interactions. © 2001 Published by Elsevier Science B.V. on behalf of the Federation of European Biochemical Societies.

Key words: Membrane restructure; Lipid-protein interaction; Gaucher's disease; Scanning probe microscopy

1. Introduction

Saposin C (Sap C), a small glycoprotein, plays an essential role in the activation of glucosylceramidase, the enzyme that degrades glucosylceramide and glucose in lysosomes [1–3]. In vitro studies showed that Sap C enhances glucosylceramidase activity in the presence of acidic phospholipid-containing membranes at acidic pHs [2,3]. A deficiency in either glucosylceramidase or Sap C results in the accumulation of glucosylceramide and leads to various forms of Gaucher's disease [1,4]. Understanding of molecular mechanisms underlying Sap

C stimulation of enzyme activity may help to better define the factors that could modulate the Gaucher's disease phenotypes, potentially contributing to improve therapeutic approaches [4,5]. The function of Sap C and its interaction with enzymes and lipids have been the subject of extensive research [1–3, 5–7]. The capacity of Sap C to stimulate enzyme activation was correlated with its capacity to interact with and perturb phospholipid membranes [6], possibly by attaching to regions in a membrane enriched in negatively charged phospholipids [5].

Much of the current knowledge of the interaction between Sap C and phospholipid membranes is based on fluorescence studies of Sap C binding, content leakage, and resonance energy transfer [2,3,5–7]. Conformational changes of Sap C, when it binds to a liposome, can be readily revealed by circular dichroism (CD) [5–7]. Electron microscopy (EM) has been used to monitor the increase in vesicle size during Sap C-induced membrane fusion [7]. However, there have been few real-time studies on dynamic behaviors of Sap C interacting with phospholipid membranes, and little evidence exists directly showing the effect of Sap C on the re-organization of phospholipid membranes [1–3].

Atomic force microscopy (AFM) is a useful technique to elucidate surface structure of biological materials at high resolution [8,9]. A major advantage of AFM is that it can be operated under aqueous and physiological conditions. The ability to perform AFM imaging in a physiological environment makes it possible to monitor important biological processes in real time at high resolution [8,9]. Currently, there is a great deal of interest in AFM studies of the interaction between proteins and supported planar lipid membranes (SPLMs), and of the role of lipids in influencing the activity of membrane-bound and/or associated proteins [10–14]. However, there are few reports on using AFM to study the dynamic processes of protein interactions with SPLMs [14], due to the intrinsic limitation of slow scan rate and of potential cantilever damage to soft biological samples [9].

Here we have used AFM to study Sap C interaction with SPLMs. Appropriate lipid membrane models offer an opportunity to study interactions between Sap C and the membrane in greater detail. The aim of our AFM study is to visualize directly the effects of Sap C on the structure of SPLMs by observing the dynamic process in real time. A better understanding of the nature and effects of the interaction between Sap C and the lipid membrane will be an important step toward delineating the mechanism of enzyme activation at the molecular level.

*Corresponding author. Fax: (1)-513-5582445.
E-mail address: hong.you@uc.edu (H.X. You).

Abbreviations: Sap C, saposin C; AFM, atomic force microscopy; DSPC, 1,2-distearoyl-*sn*-glycero-3-phosphocholine; POPS, 1-palmitoyl-2-oleoyl-*sn*-glycero-3-[phospho-L-serine]; CPS, citrate phosphate buffer; SPLM, supported planar phospholipid membrane

2. Materials and methods

2.1. Materials

All synthetic phospholipids, such as 1,2-distearoyl-*sn*-glycero-3-phosphocholine (DSPC) and 1-palmitoyl-2-oleoyl-*sn*-glycero-3-[phospho-L-serine] (POPS), were purchased from Avanti Polar Lipids (Alabaster, AL, USA) and dissolved in chloroform. Chemical reagents used for buffer solutions were purchased from Sigma (St. Louis, MO, USA). Water used was filtered with a Barnsted MilliQ Plus system (Bedford, MA, USA) with a resistance higher than 18 M Ω /cm.

2.2. Preparation of Sap C

The expression and purification of Sap C was carried out as described [15]. Briefly, the coding region for human Sap C gene was cloned into a pET vector, overexpressed in *Escherichia coli*, and purified on nickel columns. After elution from the His-Bind resin, the saposin eluates were dialyzed and lyophilized. The dried proteins were dissolved in 0.1% trifluoroacetic acid and applied to a HPLC C₄ reverse-phase column. The column was washed with 0.1% trifluoroacetic acid for 10 min, and a linear (0–100%) gradient of acetonitrile was established over a period of 60 min. The major protein peak was collected and lyophilized. Protein quantity was determined by the Lowry method using bovine serum albumin as the standard. The purity of recombinant Sap C was assessed by sodium dodecyl sulfate–polyacrylamide gel electrophoresis (SDS–PAGE) using silver staining [15] and is better than 95%.

2.3. Vesicle preparation

DSPC and POPS stock solutions in chloroform were mixed in a glass tube with a molar ratio of 10:1. The lipid mixture was dried under a flow of N₂ gas followed by incubation in vacuum for at least 45 min. To the dried lipid film was added the preparation buffer (50 mM NaCl and 20 mM Tris–HCl, pH 7.4), yielding a mixture of DSPC (8 mg/ml) and POPS (0.8 mg/ml). The mixed lipid suspension was sonicated in a bath sonicator (Fisher Scientific, Pittsburg, PA, USA) for 30–60 min. The vesicles prepared had a diameter of 150–200 nm measured using the Coulter N4 PLUS particle size analyzer (Coulter Corporation, Miami, FL, USA). The unilamellar property of the vesicles was determined by [³¹P]NMR spectroscopy in the presence of Mn²⁺ quenching [16]. The final vesicle suspension was stored at 4°C until use.

2.4. Preparation of supported planar phospholipid membranes

SPLMs were prepared by the vesicle fusion method adopted from [17]. To facilitate vesicle fusion to the negatively charged mica surface, 1% (v/v) 20 mM CaCl₂ was added to the lipid mixture solution. A piece of freshly cleaved mica was immersed in the vesicle suspension, and incubated for at least 3 h at 57°C in a water bath. The sample was let to cool down to room temperature under ambient conditions, and then washed with the preparation buffer and mounted for AFM imaging. It should be noted that the sample was always covered with a layer of the buffer during handling in order to avoid direct air contact and lipid oxidation.

2.5. Atomic force microscopy

The sample was transferred into the fluid cell of the AFM (Nanoscope IIIa, Digital Instruments Inc., Santa Barbara, CA, USA) and kept at room temperature (26 ± 1°C) in 200 mM citrate phosphate buffer (CPS: 200 mM citric acid and 200 mM di-sodiumphosphate, pH 4.7). The pH value of 4.7 was to mimic the acidic intralysosomal environment, where mature Sap C is localized [2,3]. Standard V-shaped Si₃N₄ cantilevers of 0.06 N/m force constant (Digital Instruments Inc.) were used. Samples were imaged in contact mode, with a loading force of typically ≤ 1 nN and at a scan rate of 2.54 Hz. Both height and deflection images acquired in the retrace direction were obtained from the same area.

The DSPC/POPS membrane was first surveyed under the AFM for reasonably large surface coverage. Once a desirable surface area was located, its surface topography was obtained in both height and deflection imaging formats. While continuing to scan, a Sap C solution (50 µg/ml or 100 µg/ml in CPS) was injected, using a Hamilton syringe, into the imaging buffer via the tiny gap between the sample and the AFM fluid cell. Subsequent images were recorded. Occasionally, scanning had to be abandoned because the injection of Sap C either severely distributed the thermal equilibrium of the AFM fluid cell or

induced strong interaction between the scanning tip and the sample. In such cases, a new sample was used.

3. Results

3.1. Planar phospholipid membrane forms and is stable

Activation of glucosylceramidase requires the presence of Sap C and an acidic phospholipid containing a long unsaturated fatty acid acyl chain [5]. POPS is such a phospholipid, and was chosen in this study. In general, the DSPC/POPS membrane prepared via the vesicle fusion method produces a hydrated gel-state membrane [14,17], which usually contains defects, as revealed in AFM images, commonly in the form of holes. Fig. 1 is a representative image of the DSPC/POPS membrane, with several defects (dark areas) in the membrane. Fig. 1 also highlights the stability of the membrane under continuous AFM scanning. After scanned for a period of ~79 min (Fig. 1B), no significant changes occurred in the topography of the DSPC/POPS membrane except the slight variation of the defect's shape (arrows 1 and 2 in Fig. 1B) and the removal of a small portion of the membrane by the scanning AFM cantilever (arrow 3). The thickness of the DSPC/POPS membranes is 3.66 ± 0.64 nm (*n* = 200) (Fig. 1E), consistent with pure lipid nature of the membrane without any proteins.

3.2. Sap C induces membrane restructuring

In the cell, Sap C localizes in lysosomes, and is known to attach to the lysosomal phospholipid membrane [1–4]. To examine how Sap C interacts with phospholipid membranes, Sap C was added to the planar phospholipid membrane while the membrane was continuously imaged by AFM.

Fig. 2 shows a representative set of time-lapse AFM images of the supported DSPC/POPS membrane on mica obtained before and after the addition of 50 µg/ml Sap C. The initial membrane before the addition of Sap C showed a large smooth surface (Fig. 2A). About 6 min after Sap C was injected, small islands were seen emerging at the edge of the membrane (Fig. 2B). Also, a chain of these individual structural features appeared in the lower portion of Fig. 2B and later disappeared (Fig. 2D). With time, the individual structural features grew larger (Fig. 2C and D), formed patch-like features, and eventually, the growth was substantially slowed down (Fig. 2E and F). The final horizontal size of the patches is in the range of 300–500 nm.

Sap C-induced new patches display a markedly different image contrast from the smooth planar phospholipid membrane, suggesting the formation of a new phase of lipid–protein structure. The thickness histograms (Fig. 2H and I) show that the new lipid–protein patch is about 5.78 ± 0.69 nm higher than the DSPC/POPS lipid membrane, suggesting that the Sap C-containing new structure is substantially thicker than the pure phospholipid membrane without any proteins.

3.3. Higher abundance of Sap C results in greater extent of membrane restructuring

Sap C was also used at a higher concentration (100 µg/ml) in some experiments. Representative time-lapse AFM images of the DSPC/POPS membrane on mica obtained before and after the addition of 100 µg/ml Sap C are shown in Fig. 3. Sometimes, the addition of the Sap C solution causes a physical shift in the AFM scanning area, and we rely on distinctive

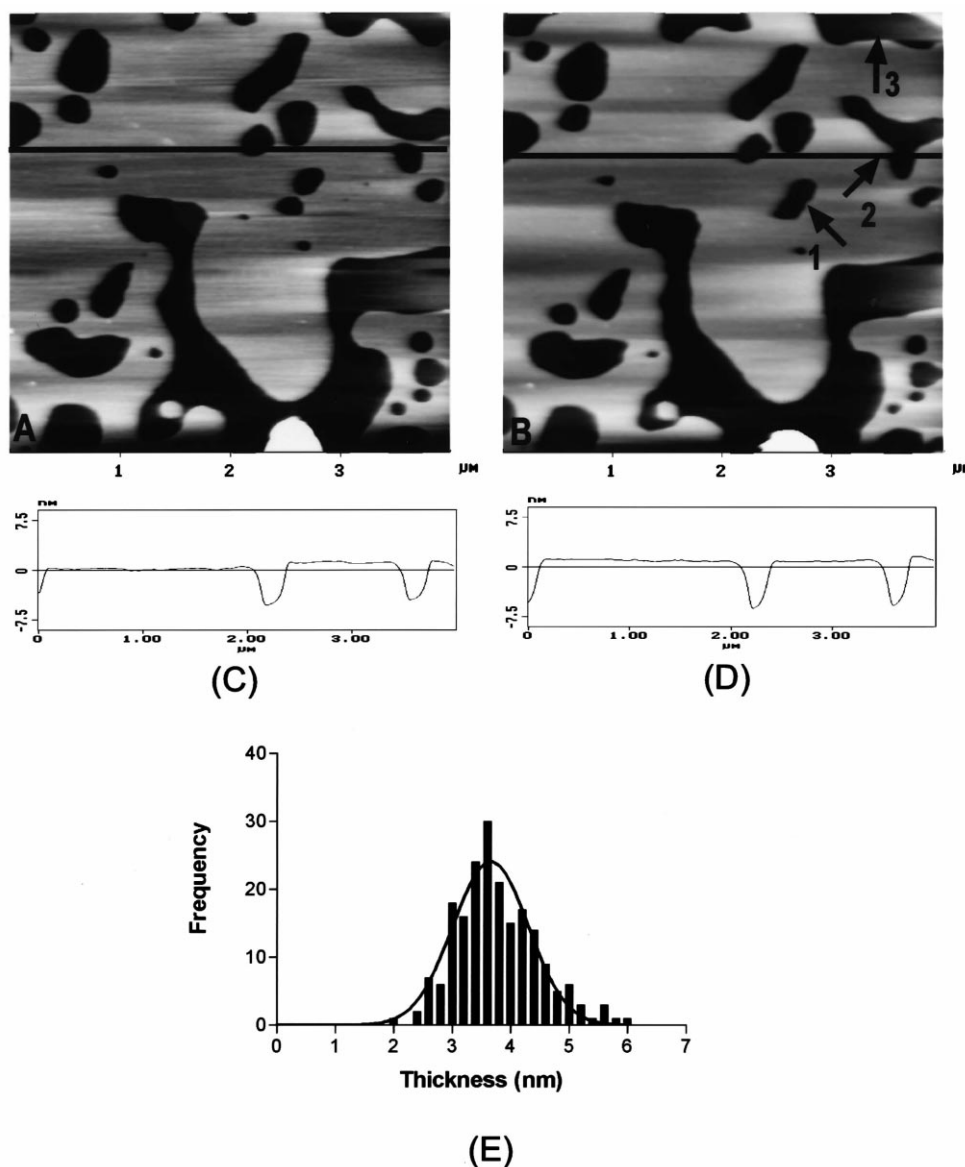


Fig. 1. Representative AFM images ($4 \times 4 \mu\text{m}$) of the supported DSPC/POPS membrane on mica, showing surface topography (A) and the stability of the membrane (B). Image (B) was obtained from the same area of (A) after being continuously scanned in the CPS for 79 min. At the upper right corner, small round defects merged (indicated by arrows 1 and 2) and a small portion of the membrane (arrow 3) was removed. The images are presented in height mode. The line profiles (C and D) were obtained, respectively, from the location as indicated by the horizontal line in A and B. The line profiles show practically no alteration of the membrane surface between the initial image (A and C) and after continuously scanned for 79 min (B and D), highlighting the stable nature of phospholipid membranes. Histogram (E) of the thickness of the supported DSPC/POPS membrane on mica. The histogram was fitted with Gaussian distribution. The membrane thickness is $3.66 \pm 0.64 \text{ nm}$ ($n = 200$).

features in the images to properly reference and align the images. The white arrow in both Fig. 3A and B indicates such a reference point for alignment of the two images. As can be seen in Fig. 3, about 7 min after the addition of the Sap C solution, small structural features similar to those in Fig. 2 started to appear at the edge of the membrane (Fig. 3B). These structural features expanded quickly, became closer to each other, and finally fused together until the surface of the DSPC/POPS membrane was mostly covered (Fig. 3C, D and E). After continuous AFM scan for ~ 25 min, certain portions of the membrane disappeared (Fig. 3F). Compared with limited sizes of restructured membrane patches in Fig. 2, the much more extensive restructured membrane area in Fig. 3 suggests that, with higher concentration of Sap C solution

(thus a higher abundance of Sap C molecules), the newly formed lipid–protein patches expand faster, resulting in greater extent of membrane restructuring. The final horizontal size of the patches is in the range of 400–800 nm.

The thickness histograms (Fig. 3H and I) show that the newly formed patch-like features are about $4.06 \pm 0.86 \text{ nm}$ higher than the surface of the pure phospholipid membrane, again suggesting that the new lipid–protein phase is substantially thicker than the pure membrane without any proteins.

Other phenomena observed during the membrane restructuring processes include: (i) the formation of the patch-like features shows that the edge of the planar phospholipid membrane is the preferential starting site; (ii) the growth of the patch-like features is laterally within the phospholipid mem-

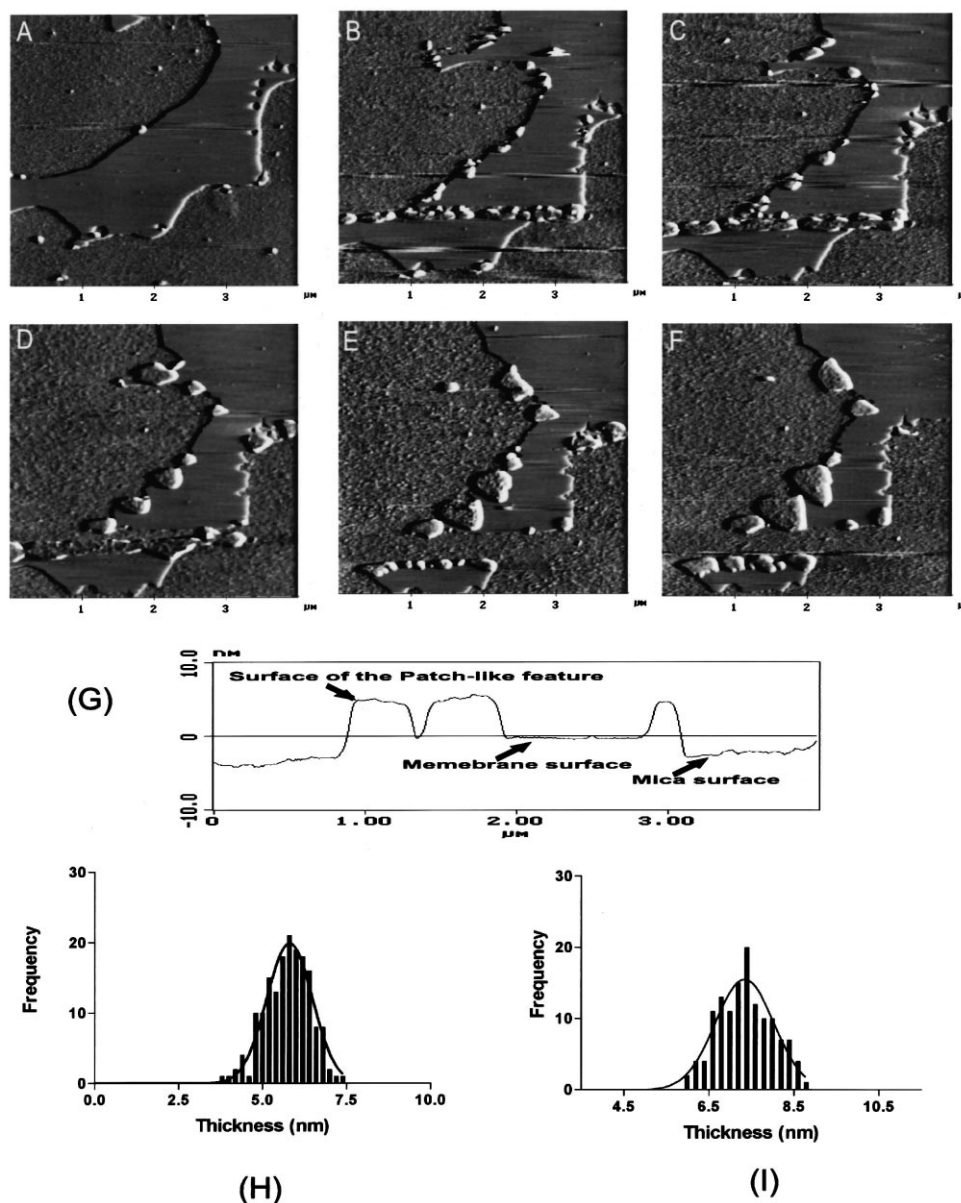


Fig. 2. A representative time sequence of AFM images of the DSPC/POPS membrane on mica showing Sap C-induced membrane restructuring. (A) Prior to Sap C addition, and (B) 6 min, (C) 9 min, (D) 16 min, (E) 29 min, (F) 44 min, respectively, after the addition of 50 $\mu\text{g}/\text{ml}$ Sap C solution into the AFM fluid cell. The images were obtained in the CPS and presented in deflection mode. At the end of each scanning frame, a force–distance curve was taken and the loading force was adjusted, if necessary, back to less than 1 nN. Notice the different image contrast between the smooth phospholipid membrane and the rough surface of newly formed patches. Images size: $4 \times 4 \mu\text{m}$. The line profile (G) was measured from the corresponding height image at the same location as indicated by a white horizontal line in F. The histogram (H) of the thickness of the patch-like features measured as the height difference between the top surface of the patch-like features and the membrane surface. The histogram (I) of the total thickness measured as the difference in height between the top surface of the patch-like features and the mica surface. The histograms were fitted with Gaussian distribution. The thickness of the patch-like features is $5.78 \pm 0.69 \text{ nm}$ ($n = 169$) and the total thickness is $7.34 \pm 0.68 \text{ nm}$ ($n = 131$). In AFM, an error signal is generated by the cantilever deflection via a position photodetector. This signal is used to control the feedback loop and converted to display as true height. The image obtained thereafter is called the height image, which contains topographic information. However, the error signal can be used directly to display without any conversion, and the image obtained is the deflection image. The deflection image enhances high frequency components in the image and offers improved contrast for high-resolution imaging.

brane-covered area, and not on bare mica where no phospholipid membrane exists; and (iii) the patch-like features are stable under the experimental conditions and contain no obvious defects.

3.4. Adsorption of Sap C on mica

The adsorption of Sap C on bare mica was carried out to

determine the height of Sap C molecules. A drop ($\sim 20 \mu\text{l}$) of 25 $\mu\text{g}/\text{ml}$ Sap C in CPS (pH 4.7) was deposited on freshly cleaved mica, and the sample was left at room temperature for $\sim 1 \text{ h}$ before imaged in the CPS (pH 4.7). Sap C molecules on mica tended to form rod-like features. The height of Sap C molecules, measured as the thickness of the rod-like features, was $1.77 \pm 0.55 \text{ nm}$ ($n = 76$).

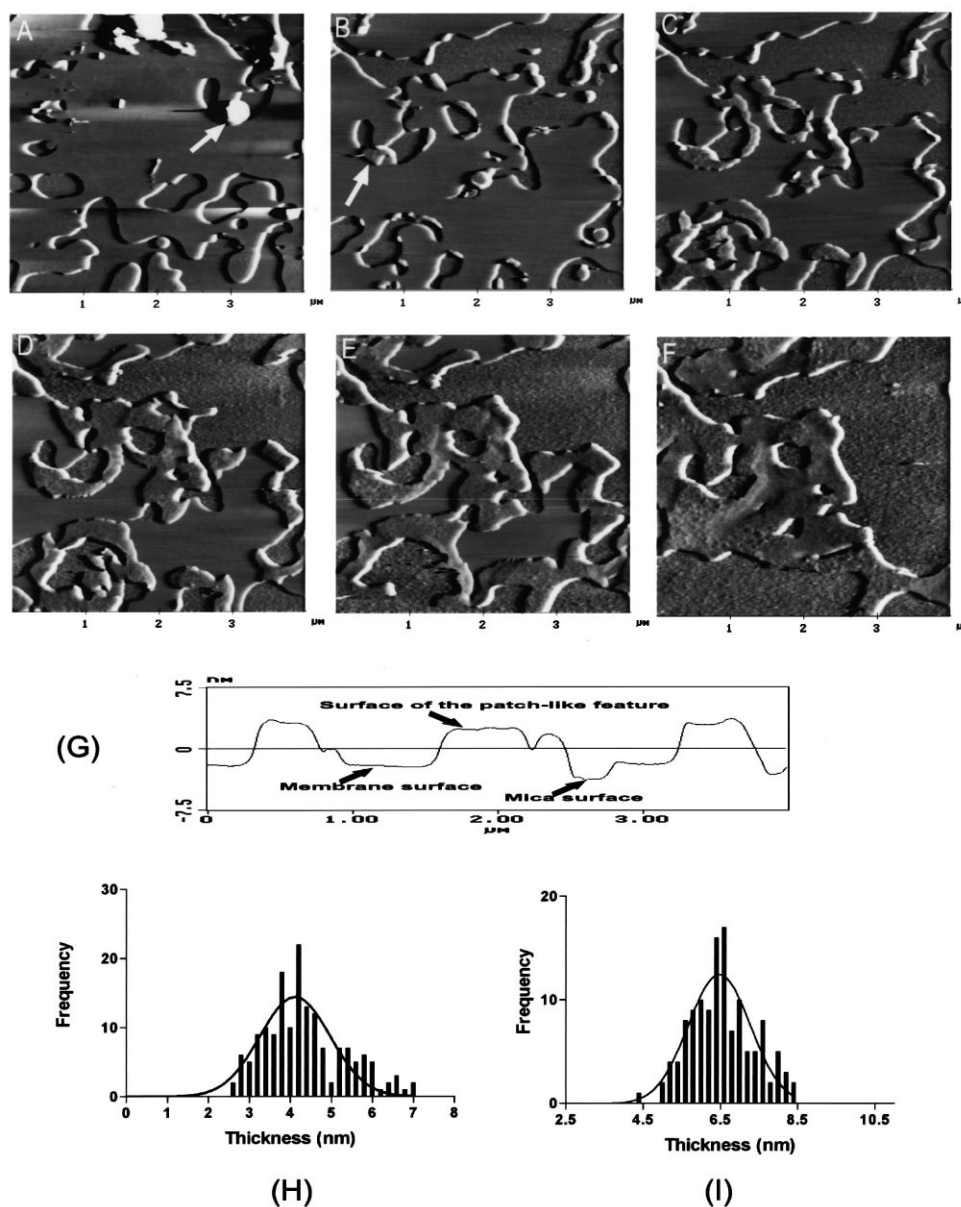


Fig. 3. Representative time-lapse series of AFM images of the DSPC/POPS membrane on mica showing greater extent of membrane restructuring induced by higher Sap C concentration. (A) prior to Sap C addition, and (B) 7 min, (C) 10 min, (D) 14 min, (E) 17 min, (F) 25 min, respectively, after the addition of 100 $\mu\text{g/ml}$ Sap C solution into the AFM fluid cell. The scanning was conducted in the CPS and the images are presented in deflection mode. The position pointed by a white arrow in A and B serves as a reference point for aligning images before and after Sap C addition, which causes a shift in the AFM scanning area. Image size: $4 \times 4 \mu\text{m}$. The line profile (G) was measured from corresponding height image at the same location as indicated by a white horizontal line in E. The histogram (H) of the thickness of the patch-like features measured as the height difference between the top surface of the patch-like features and the membrane surface. The histogram (I) of the total thickness measured as the difference in height between the top surface of the patch-like features and the mica surface. The histograms were fitted with Gaussian distribution. The thickness of the patch-like features is $4.06 \pm 0.86 \text{ nm}$ ($n=164$) and the total thickness is $6.46 \pm 0.84 \text{ nm}$ ($n=127$).

4. Discussion

The three-dimensional molecular structure of Sap C is unknown at present [2,3]. Even though the three-dimensional structure of monomeric NK-lysin, a saposin-like protein, was determined recently [18], how lipid membranes may interact with such proteins is unclear [19]. In the present study, we employed AFM to examine protein–membrane interaction, and were able to observe the dynamic process of the interaction in real time.

We first determined that, in the absence of Sap C, the

SPLM of DSPC/POPS on mica was very stable, with virtually no alteration even after continuous AFM scanning for over an hour (Fig. 1). This fact establishes that structural changes observed by AFM in subsequent experiments must be due to the additional manipulation (i.e. the addition of Sap C proteins).

When Sap C was introduced to the otherwise stable DSPC/POPS membrane, we observed a process of dynamic restructuring (Figs. 2 and 3). Patch-like features were formed, and the sizes of these patches continued to increase over most of the AFM scanning duration, highlighting the dynamic nature

of such membrane restructuring. The extent of the patch growth appears to be related to protein abundance, as lower Sap C concentration produces fewer patches with smaller sizes (Fig. 2), while higher Sap C concentration results in much larger patches, sometimes covering the entire regions of the DSPC/POPS membrane (Fig. 3).

The newly formed lipid–protein patches after membrane restructure are rather thick, protruding additional 4–5 nm above the pure phospholipid membrane (Figs. 2 and 3). Sap C is a small protein containing 80 amino acids. The height of Sap C molecules absorbed on bare mica was measured at 1.77 ± 0.55 nm using AFM. Considering these, it remains to be determined the organization of the restructured lipid–protein phase. There are reports of Sap C-induced fusion of phosphatidylserine (PS)-contained liposomes at acidic pHs [2,3,7]. It has been suggested that once Sap C is bound to a lipid membrane, its solvent-exposed top half is able to interact with another liposome-bound Sap C [2,19]. In the experiment, we have attempted to inject Sap C solution, for the second time, into the AFM liquid cell after the DSPC/POPS surface was completely covered by the patch-like features from the first Sap C injection. However, we did not observe further expansion of already formed lipid–protein patches, either in size horizontally or in thickness vertically (data not shown). Further experiments are needed to explain the dramatic changes in the membrane topography occurred in the presence of Sap C. On the other hand, the remarkable difference found in image contrast between the patch-like features and the pure DSPC/POPS membrane suggests a new phase of structure formed.

The patch-like features show preferential formation at the edge of the lipid membrane where the phospholipids are not well packed, and spread only along the surface of the DSPC/POPS membrane. In the DSPC/POPS gel phase regions (i.e. the smooth area of the membrane), where the phospholipids are well organized, we seldom observed the initiation of membrane restructuring. The preferential formation of the patch-like features at the edge of the membrane may thus reflect structural differences within membrane organization: the curvature at the edge of lipid membranes reduces the lipid packing, and thus increases the accessibility of the POPS, the reactive components of the membrane in our samples, to Sap C [14]. Sap C binding to POPS further disturbs local organization of the membrane and makes more POPS accessible. This manifests the growth of the patch-like features always extending from the edge of the membrane and along its surface.

Real-time structural studies of protein–membrane interactions in physiological solution at high resolution are a challenge, which at present can be accomplished only by AFM. The results of our work demonstrate the capacity of using AFM to study the dynamic process, in real time, of phospholipid membrane restructuring. Future studies with this approach should contribute to a better understanding of protein–membrane interaction.

Acknowledgements: We thank Ms. J. Lau and Dr. J. Strong for critical review of the manuscript. This work was supported in part by NIH grants DA09444, DA11891, and DA12848 (L.Y.) and DK57690 (X.Q.).

References

- [1] O'Brien, J. and Kishimoto, Y. (1991) *FASEB J.* 5, 301–308.
- [2] Qi, X. and Grabowski, G.A. (2000) *Prog. Nucleic Acid Res. Mol. Biol.* 66, 203–239.
- [3] Vaccaro, A.M., Salvioli, R., Tatti, M. and Ciaffoni, F. (1999) *Neurochem. Res.* 24, 307–314.
- [4] Grabowski, G.A. and Horowitz, M. (1997) *Baillieres Clin. Haematol.* 10, 635–656.
- [5] Qi, X. and Grabowski, G.A. (1998) *Biochemistry* 37, 11544–11554.
- [6] Vaccaro, A.M., Ciaffoni, F., Tatti, M., Salvioli, R., Barca, A., Tognozzi, D. and Scerch, C. (1995) *J. Biol. Chem.* 270, 30576–30580.
- [7] Vaccaro, A.M., Tatti, M., Ciaffoni, F., Salvioli, R., Serafino, A. and Barca, A. (1994) *FEBS Lett.* 349, 181–186.
- [8] Lal, R. and John, S.A. (1994) *Am. J. Physiol.* 266, C1–C21.
- [9] You, H.X. and Yu, L. (1999) *Methods Cell Sci.* 21, 1–17.
- [10] Bayburt, T.H., Carlson, J.W. and Sligar, S.G. (1998) *J. Struct. Biol.* 123, 37–44.
- [11] Santos, N.C., Ter-Ovanesyan, E., Zasadzinski, J.A. and Castanho, M.A. (1998) *Biophys. J.* 75, 1869–1873.
- [12] Rinia, H.A., Kik, R.A., Demel, R.A., Snel, M.M., Killian, J.A., van der Eerden, J.P. and de Kruijff, B. (2000) *Biochemistry* 39, 5852–5858.
- [13] Zuber, G. and Barklis, E. (2000) *Biophys. J.* 78, 373–384.
- [14] Grandbois, M., Clausen-Schaumann, H. and Gaub, H. (1998) *Biophys. J.* 74, 2398–2404.
- [15] Qi, X., Leonova, T. and Grabowski, G.A. (1994) *J. Biol. Chem.* 269, 16746–16753.
- [16] Qi, X. and Grabowski, G.A. (2001) *J. Biol. Chem.*, in press.
- [17] Brian, A.A. and McConnell, H.M. (1984) *Proc. Natl. Acad. Sci. USA* 81, 6159–6163.
- [18] Liepinsh, E., Andersson, M., Ruyschaert, J.M. and Otting, G. (1997) *Nat. Struct. Biol.* 4, 793–795.
- [19] Ruyschaert, J.-M., Goormaghtigh, E., Homble, F., Andersson, M., Liepinsh, E. and Otting, G. (1998) *FEBS Lett.* 425, 341–344.